A Robotic Device for Manipulating Human Stepping

Jeremy L. Emken, John H. Wynne, Susan J. Harkema, and David J. Reinkensmeyer

***Abstract*—This paper provides a detailed design description and technical testing results of a device for studying motor learning and rehabilitation of human locomotion. The device makes use of linear motors and a parallel mechanism to achieve a wide dynamic force bandwidth as it interacts with the leg during treadmill stepping.**

***Index Terms*—Linear motor, locomotion, motion measurement, robots.**

I. Introduction

An emerging area of robotics research is the development of robotic devices to study human motor learning, both in healthy people in order to understand the fundamental mechanisms of motor adaptation, and in neurologically injured patients, with the goal of manipulating those mechanisms in order to facilitate rehabilitation [1]–[3]. Robotic devices allow experimenters to apply novel dynamic environments to the limbs in a repeatable way, allowing for a controlled examination of the learning and recovery processes.

Devices used to study motor learning and rehabilitation of the upper limb include an industrial robot [4], a force-feedback controlled haptic robot [5], devices combining passive and active degrees of freedom (DOFs) [6], and a cable-driven haptic robot [7]. The mostly widely used robot type uses two large, mechanically grounded motors to drive a lightweight, four-bar parallelogram configuration [1], [8], [9] or pantograph [10] linkage in a horizontal plane, thereby achieving both large forces and good backdrivability. This design has been used in pioneering studies of robot-assisted movement therapy for the arm following a stroke, and in a large number of influential motor adaptation studies (see reviews in [1] and [3]).

Robotic devices have also been designed for studying human walking and for employing rehabilitation approaches after neurologic injury [11]–[15]. A recent focus of these devices has been automating a promising rehabilitation technique known as locomotor training, which uses step training with body-weight support on a treadmill (BWST) [16]. In this technique, the patient's body weight is partially supported with a hoist, and therapists manually assist the patient's legs and torso. The technique has been suggested to modulate neural circuits in the spinal cord by providing appropriate patterns of sensory input [17], and has been shown to improve over ground walking ability in patients with spinal cord injury (SCI) and stroke [18], [19]. The technique has remained relatively inaccessible in rehabilitation clinics because it is highly labor-intensive, requiring two to three skilled trainers to manually assist the patient's hips and legs.

Several groups have developed devices for automating locomotor training [12], [15], [20]. The Mechanized Gait Trainer (MGT) is a singly actuated mechanism that drives the feet through a gait-like trajectory using a doubled crank and rocker system [20]. The Lokomat is a motorized exoskeleton that has four rotary joints that drive hip and knee flexion/extension for each leg [15]. The joints are driven in a gait-like pattern by precision ball screws connected to DC motors [15]. The HapticWalker, a newer design from the MGT group, uses linear and rotary motors to control the position of two foot plates, simulating the ground moving beneath a subject [12].

While these locomotor robots are capable of driving the legs through a gait-like pattern, they are relatively limited in their dynamic bandwidth. The MGT cannot drive the legs away from the path specified by its single DOF mechanical linkage. The Lokomat is difficult to backdrive, because it uses high-advantage ball-screw actuators. The HapticWalker has relatively large, high-inertia robotic arms that support the patient's weight, and this apparent inertia must be reduced using force feedback.

Ideally, there would exist a robotic device that allows a wide dynamic range of forces to be applied to the leg during naturalistic gait movements, maximizing the potential number of dynamic environments available to study motor learning and promote motor rehabilitation. For example, it is desirable for a gait-training robot to be able to reduce the amount of assistance it provides as a patient recovers, such that it "fades to nothing." One approach to achieving the large dynamic bandwidth required for "assistance as needed" is to use force feedback or admittance control. Following initial clinical testing, the Lokomat group is currently trying to improve the dynamic bandwidth of their devices using force-control methods [21]. Another approach is to develop a mechanism that is inherently backdrivable, yet still allows for high force generation. A logical candidate mechanism is the same four-bar mechanism described above that has been successful in arm movement studies. However, this approach would be difficult to apply to humans, because the forces required to move the legs are relatively large compared with the arms, and would necessitate either extremely large motors, or smaller geared motors, working against the backdrivability advantage of this mechanism.

This paper provides a detailed design description and technical testing results of a direct-drive parallel device with a high dynamic bandwidth that can be used to mechanically interact with the leg during treadmill stepping. The main significance of this work is that it is possible to create a highly responsive gait robot using only simple control strategies, given this mechanism design. Examples of the device's ability to assist in stepping, and to induce motor adaptation by creating a novel dynamic environment, are given.

II. Methods

A. Mechanical Design

The locomotor robot consists of two moving coil brushless linear servomotors that drive either end of a two-bar linkage in the parasagittal plane (Fig. 1). The linkage apex is attached through a revolute joint that can be attached to the lower limb at the knee, ankle, or bottom of the foot through custom composite braces. The apex can be moved in any desired planar trajectory $x(t)$, $y(t)$ by moving the linear motors along trajectories $x_1(t)$ and $x_2(t)$, specified by

$$x_1(t) = x(t) + \sqrt{l^2 - y^2(t)}$$
$$x_2(t) = x(t) - \sqrt{l^2 - y^2(t)} \quad (1)$$

Manuscript received February 4, 2005; revised August 30, 2005. This paper was recommended for publication by Associate Editor J. Troccaz and Editor F. Park upon evaluation of the reviewers' comments. This work was supported in part by the NIST under ATP 00-00-4906, in part by the NCRR under M01RR00827, and in part by an ARCS Foundation Scholarship to the first author. This paper was presented in part at the Second Joint Meeting of the IEEE Engineering in Medicine and Biology Society and the Biomedical Engineering Society, Houston, TX, October 2002.

J. L. Emken is with the Biomedical Engineering Department, University of California at Irvine, Irvine, CA 92697 USA (e-mail: jemken@uci.edu).

J. H. Wynne and D. J. Reinkensmeyer are with the Mechanical and Aerospace Engineering Department, University of California at Irvine, Irvine, CA 92697 USA (e-mail: dreinken@uci.edu).

S. J. Harkema is with the Neurology Department, University of California at Los Angeles, Los Angeles, CA 90095 USA.

Digital Object Identifier 10.1109/TRO.2005.861481

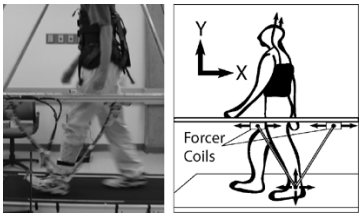

Fig. 1. Picture (left) and diagram (right) of experimental setup. The robot makes use of a linear motor with two forcer coils and a V-shaped linkage to accommodate and drive apex motion in the parasagittal plane. The apex is attached through a padded cuff and revolute joint to the subject's ankle.

where l is the length of each link. The link lengths that work well for the knee, ankle, and bottom of foot configurations were 18, 53, and 57 cm, respectively. In addition, the height of the linear rail can be easily changed to adjust the device workspace. The planar force F_x, F_y applied by the apex to the leg is controlled open loop by applying forces F_1 and F_2 with the linear motors

$$F_1 = 0.5F_x + \frac{(x_2 - x_1)}{4\sqrt{l^2 - \left(\frac{x_2 - x_1}{2}\right)^2}}F_y$$
$$F_2 = 0.5F_x - \frac{(x_2 - x_1)}{4\sqrt{l^2 - \left(\frac{x_2 - x_1}{2}\right)^2}}F_y. \quad (2)$$

This mechanism design has several advantages. A moving coil linear motor can generate substantial force, yet has low backdrive friction, so the device is powerful yet lightweight. In addition, force application can be mechanically constrained to a physical workspace that matches the legs during walking with simple hard stops or by installing short links. When compared with exoskeletal approaches, the device is more flexible, as it can accommodate any size leg and any step trajectory without the need for mechanical adjustments.

B. Hardware and Software Development

We have built a prototype of this device design called "ARTHuR"(Ambulation-assisting Robotic Tool for Human Rehabilitation) (Fig. 1), for interacting with one leg during stepping. The basic design parameters specified that the device would be able to lift a large leg ($\sim$ 150 N vertical force), accommodate a large step size, and have a force bandwidth at least twice that of human stepping ($\sim$ 2 Hz bandwidth) while remaining as lightweight as possible. To satisfy the force requirements, ARTHuR's power is derived from two moving coil forcers (Baldor, DC brushless linear motors: LMCF04C-HC0 controlled by two Baldor LinDrives: LD1A02TR-EN20), each with a mass of 0.32 kg and a peak and continuous force capability of 173 and 58 N. In endpoint coordinates with the device at a configuration typical for stepping (apex angle of 60°), this allows peak horizontal and vertical forces of 346 and 600 N, respectively. The continuous-endpoint horizontal and vertical forces are approximately one-third of peak, and are thus equal to 116 and 200 N in the x and y directions. In continuous output, this force capability is about the same as that measured from physiotherapists manually stepping a severely injured SCI subject [23]. Position of the moving coils is measured using a linear optical encoder with one read head (Renishaw, RGH41) per coil at a resolution of 20 μm. The encoder read heads are capable of measurements up to 12 m/s. Each coil rides along a linear roller bearing (THK, HSR-15R) attached to a single 2-m length of rail. With the attachment at the foot or ankle, this allows a trapezoid-shaped workspace 0.55 m high, with a 1.72 m base and 0.71 m top. This workspace accommodates typical ankle trajectories with stride lengths of 0.6 m and step heights of 0.2 m. The system is controlled using MATLAB's Simulink (The Mathworks, Inc.) and xPC Target operating at 1000 Hz along with an encoder board (Addi-Data APCI1710), a digital/analog IO Board (Computer Boards PCIM-DDA06-16), and an OOPic II (Savage Innovations).

Static backdrive friction due to the ball bearing-rail interface was measured to be approximately 3.4 N for each coil. Dynamic friction, which was measured to be approximately 2.3 N $\cdot$ s/m, is cancelled through software by creating an assistive force proportional to the velocity of each coil. In addition, the weight of the linkage and attached brace are cancelled in the software, so as not to gravitationally load the limb. In order to minimize the device's apparent inertia, the linkages and the apex with brace have been made as lightweight as possible. We estimated the device's inertia by measuring the position-control response to sinusoidal inputs across a range of frequencies, with the device in a typical stepping configuration. The apparent inertia in the horizontal and vertical directions was 4.2 and 7.2 kg.

Safety is obviously of paramount importance for robotic devices that physically interact with humans. Operating along with the control program at 1000 Hz are several safety checks, each of which creates a fault condition that stops both the robot and the treadmill. Position-limit checks monitor coil and endpoint positions to verify that they are within a safe workspace. Coil and endpoint velocity-limit checks detect if the subject has moved excessively fast, sensing a fall or trip. Force limits saturate excessive coil and resultant endpoint force. The motor drivers verify proper operation of the encoders, hall effect sensors, and motor coils, and produce a fault if an error is sensed. An independently powered watchdog timer checks for system crashes of the target computer. An emergency stop button is held during operation. We considered using a mechanical method to disconnect the user from the device if forces became too high [4], but did not use this approach, because we were concerned that the disconnected robot's momentum could cause a collision with the subject's leg. Finally, all subjects wear a support harness attached to an overhead frame to catch them if they fall.

C. Experimental Testing

To verify the robot's capabilities, we characterized its force-control ability, backdrivability, position-tracking ability, and force-field generation capability. To test how accurately the end-effector could exert commanded forces, we recorded output forces from the device at 50 Hz using a six-axis force transducer (Industrial Automation, Theta) in three experiments. During all experiments, ARTHuR was attached through a revolute joint to the force transducer at an apex angle of 60°. In the first experiment, we tested the directional accuracy of ARTHuR when commanded to produce a constant force of 22.2 N in 12 equally spaced directions around a circle. In a second experiment, we tested the force accuracy as ARTHuR created a circle in force space at six different force magnitudes (10, 20, 40, 60, 80, and 100 N). In a third experiment, we tested the force bandwidth of ARTHuR by commanding vertical endpoint sinusoidal forces of 80 and 100 N for frequencies ranging from 0.5 to 30 Hz.

To assess the backdrivability of ARTHuR, we measured how the device perturbed stepping trajectories when two healthy adult subjects, a small female (1.3 m, 570 N) and large male (1.9 m, 900 N), stepped on the treadmill at 0.9 m/s, with the device attached around the ankle actively cancelling dynamic friction and gravity, compared with when they stepped without the device attached. A location on the subject's heel, approximately 5 cm below the lateral malleolus, was hand-digitized from digital video recorded at 30 Hz.

To test the ability of ARTHuR to record and replay a step trajectory, we recorded ankle position at 200 Hz from the same large male subject walking at 0.9 m/s on the treadmill, and then actively tracked the reproduced trajectories with a proportional-derivative (PD) controller. The subject first stepped for 50 steps with the device applying only friction and gravity cancellation. After recording the step trajectories,

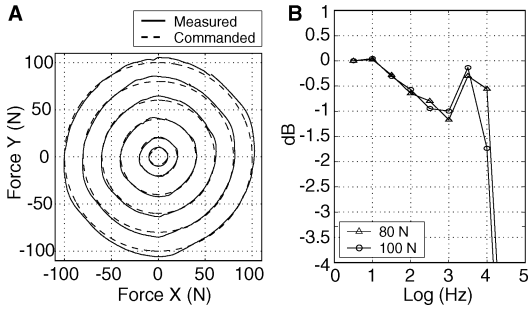

Fig. 2. Force-control tests. A: ARTHuR was commanded to produce a circle pattern in force space with force radii of 10, 20, 40, 60, 80, and 100 N. Solid line indicates commanded force and dashed line indicates the force transducer measurement. B: Magnitude of frequency response of ARTHuR for a commanded vertical sinusoid at a linkage apex angle of 60° at two force levels of 80 and 100 N.

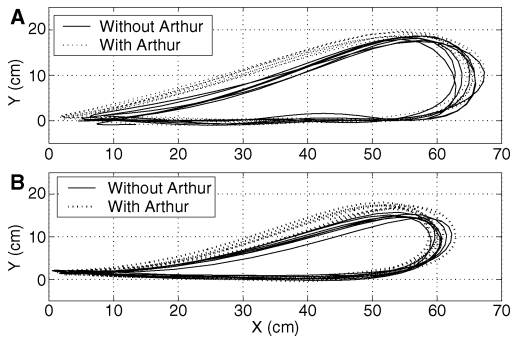

Fig. 3. Backdrivability test of ARTHuR. Step trajectories measured with video capture for a point on the ankle with and without ARTHuR attached. Seven steps are shown for each case. A: Tall male subject. B: Short female subject.

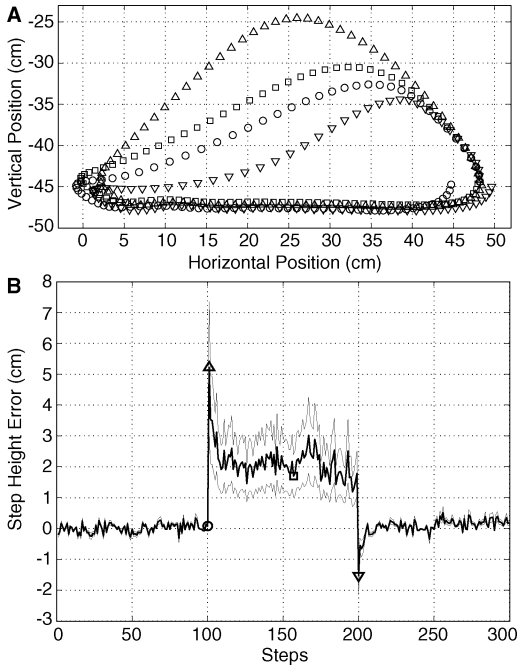

Fig. 4. Test of ARTHuR's ability to induce motor adaptation by creating a novel dynamic environment during stepping. Data is from six unimpaired subjects who stepped in the force field. For this figure, the force field was turned "on" at step 101 and "off" at step 201. A: Representative step trajectories of the lower shank for a single subject. Shown are the normal stepping trajectory in the null field (∘); the "direct effect," which is the first step in force field (△); a step produced after adaptation to field exposure (□); and the "aftereffect," which is the first step in the null field (▽). B: Mean step height error with SE lines (grey) measured mid-step referenced to the normal stepping height mid-step, before, during, and after application of the force field.

we identified the individual steps using zero crossings in horizontal velocity, and calculated a representative mean stepping trajectory. We used this averaged spatio–temporal data as our control input "desired trajectory," and measured tracking error for an endpoint coordinate, PD controller (stiffness$_{\mathrm{x\,dir}}$ $=$ 7004 N/m, stiffness$_{\mathrm{y\,dir}}$ $=$ $10\,507$ N/m, damping $=$ 350 Ns/m) with and without the mass of the subject's leg hanging in the device.

To test the functionality of ARTHuR as a tool to study motor adaptation, we replicated a seminal motor adaptation experiment [24]. In this experiment, subjects were required to adapt to a novel viscous force field while reaching between points in space. Our replication experiment required subjects to adapt to a novel viscous force field applied during the swing phase of gait while treadmill stepping. To establish a baseline stepping performance, we allowed unimpaired subjects (N = 6, age 25–37 yr, five male) to practice walking with the robot attached around the ankle for 200 steps, and then recorded step trajectories in a null field (no field applied) for 100 steps. We then commanded ARTHuR to produce a viscous force field that pushed upwards during the swing phase with a force proportional to the horizontal velocity of the robot's apex for 100 steps. The force was only applied when the robot was moving forward. We chose the proportionality constant (33–56 Ns/m) to induce a peak force equal to 8% of the subject's body weight, which was sufficient to perturb stepping, but did not induce stumbling. After applying the force field, we returned to the null field for 100 steps. We characterized the subjects' adaptation by examining step height mid-swing (300 ms after toe off) before, during, and after force field application.

III. Results

For the first force-control test, ARTHuR produced the commanded constant force of 22.2 N with an average directional error of $-0.7^{\circ} \pm 1.0^{\circ}$. ARTHuR also accurately produced a circular pattern in the force space at six different levels of force, with an average force error of -0.16 N± 1.75 N [Fig. 2(a)]. ARTHuR's bandwidth for tracking an 80 and 100 N vertical sinusoidal force was approximately 4 Hz [Fig. 2(b)]. Above 4 Hz, the structure supporting the linear motor began to resonate, limiting tracking accuracy. For comparison, we measured the frequency content of the stepping trajectory for a single subject at a cadence of 45 steps/minute, and found 90% of the power spectral density to be below 1 Hz.

For the test of its backdrivability, ARTHuR did not substantially perturb stepping trajectories when attached to the leg, compared with stepping without the device attached, for both the small and large subject [Fig. 3(a) and (b)]. The mean difference between the peak step trajectory with and without ARTHuR attached for seven digitized steps was 2.3 and 0.83 cm for the small and large subjects, respectively. There was a small tendency in both subjects to step slightly higher with the device attached to their leg, likely an "overshoot" due to the added inertia and the rapid vertical acceleration of the leg at the beginning of the swing phase of gait.

To test the device's ability to assist in movement, we recorded normal stepping trajectories, and then replayed them with ARTHuR in a position-controlled mode with and without a subject suspended from an overhead frame. ARTHuR reproduced the recorded steps with a mean tracking error of 0.74 mm without the subject attached, and 2.8 mm with the subject's limb hanging relaxed in the device.

Finally, we tested the ability of ARTHuR to induce motor adaptation by applying a velocity-dependent force field during stepping. The robot pushed the leg upward when the force field was first turned on [Fig. 4(a)] creating a "direct effect." The subjects then adapted to

the force field, reducing their step height over the course of several steps [Fig. 4(b)]. When the force field was unexpectedly removed, the subjects exhibited an "aftereffect," stepping significantly lower than null baseline for several steps before returning to the normal baseline (Fig. 4(a) and (b), ttest: $p< 0.0001$, comparing aftereffect with null baseline). The presence of the aftereffect following adaptation indicates that the subjects had learned to predict the field through the formation of an internal model of the field's dynamics.

IV. Discussion

Robotic technology has significant potential to further the scientific understanding of locomotor control and to automate locomotor training following neurologic injuries, such as SCI and stroke. A key goal in developing robotics for human-locomotion science and rehabilitation is wide dynamic bandwidth; a device with a wide dynamic bandwidth could measure stepping ability in a backdrivable mode, assist stepping in a position-controlled mode, and enhance motor adaptation by creating novel dynamic environments.

The device described here has a wide dynamic bandwidth that is achieved through a simple mechanical and control design. It can generate peak forces around 350 N at a rate up to 4 Hz, a bandwidth that is approximately quadruple that of human walking. This performance is accomplished through feedforward control and good backdrivability, rather than force feedback control, which would require the added cost of force sensors as well as increased control complexity. The device does not substantially impede stepping when attached. In position-controlled mode, the device can accurately drive a passive leg through a normative stepping trajectory. Finally, the device can generate a novel force field environment that induces locomotor adaptation.

Future research with the device will focus on three areas. First, we will use the device to assist in step training with body-weight support for SCI patients. A key issue here will be to design a controller for the device that intelligently assists in leg movement, allowing the patient to contribute as much as possible to the movement, and normalizing sensory input into the spinal cord.

A second goal is to use ARTHuR to understand how the nervous system processes sensory input to control stepping. ARTHuR can precisely grade forces applied to the knee, ankle, or bottom of the foot during swing and stance, and thus provides a new tool for examining the input–output relationship of locomotor control.

Third, we are using ARTHuR to understand locomotor adaptation to novel dynamic environments. The finding that healthy subjects form internal models of the leg's stepping environment, similar to upper extremity control, suggests that similar neural systems are involved in adaptive control of reaching and stepping. We have developed a computational model that captures the dynamics of trajectory evolution during stepping and reaching [25]. We recently used this model to demonstrate that it is possible to accelerate motor learning in a novel dynamic environment by transiently increasing trajectory errors using ARTHuR [26]. This result is, to our knowledge, the first direct evidence that a robotic device can help a person to learn a motor task more rapidly. By understanding how neurologic injuries themselves are akin to perturbing, dynamic environments, we hope to devise similar strategies for robotically accelerating motor rehabilitation.

Acknowledgment

The authors gratefully acknowledge helpful conversations with K. Day and V. R. Edgerton of UCLA, and the assistance of W. Timoszyk and C. Takahashi.

References

[1] N. Hogan and H. I. Krebs, "Interactive robots for neuro-rehabilitation," *Restor. Neurol. Neurosci.*, vol. 22, no. 3-5, pp. 349–358, 2004.

[2] S. Hesse, H. Schmidt, C. Werner, and A. Bardeleben, "Upper and lower extremity robotic devices for rehabilitation and for studying motor control," *Current Opinions Neurobiol.*, vol. 16, no. 6, pp. 705–710, 2003.

[3] D. J. Reinkensmeyer, J. L. Emken, and S. C. Cramer, "Robotics, motor learning, and neurologic recovery," *Ann. Rev. Biomed. Eng.*, vol. 6, pp. 497–525, Apr. 2004.

[4] P. S. Lum, C. G. Burgar, and P. C. Shor, "Evidence for improved muscle activation patterns after retraining of reaching movements with the MIME robotic system in subjects with post-stroke hemiparesis," *IEEE Trans. Neural Syst. Rehab. Eng.*, vol. 12, no. 2, pp. 186–194, 2004.

[5] W. S. Harwin, "Robots with a gentle touch: Advances in assistive robotics and prosthetics," *Technol. Health Care*, vol. 7, no. 6, pp. 411–417, 1999.

[6] D. J. Reinkensmeyer, L. E. Kahn, M. Averbuch, A. N. McKenna-Cole, B. D. Schmit, and W. Z. Rymer, "Understanding and treating arm movement impairment after chronic brain injury: Progress with the ARM Guide," *J. Rehab. Res. Devel.*, vol. 37, no. 6, pp. 653–662, 2000.

[7] C. D. Takahashi, R. A. Scheidt, and D. J. Reinkensmeyer, "Impedance control and internal model formation when reaching in a randomly varying dynamical environment," *J. Neurophysiol.*, vol. 86, no. 2, pp. 1047–51, 2001.

[8] S. H. Scott, "Apparatus for measuring and perturbing shoulder and elbow joint positions and torques during reaching," *J. Neurosci. Methods*, vol. 89, no. 2, pp. 119–127, 1999.

[9] R. Shadmehr and T. Brashers-Krug, "Functional stages in the formation of human long-term motor memory," *J. Neurosci.*, vol. 17, no. 1, pp. 409–419, 1997.

[10] D. W. Franklin, R. Osu, E. Burdet, M. Kawato, and T. E. Milner, "Adaptation to stable and unstable dynamics acheived by combined impedance control and inverse dynamics model," *J. Neurophysiol.*, vol. 90, no. 5, pp. 3270–3282, 2002.

[11] A. Fattah and S. K. Agrawal, "Gravity balancing rehabilitative robot for the human legs," in *Proc. 26th Annu. Int. Conf. IEEE EMBS*, San Francisco, CA, Sep. 2004, pp. 2695–2698.

[12] H. Schmidt, D. Sorowka, S. Hesse, and R. Bernhardt, "Robotic walking simulator for neurological gait rehabilitation," in *Proc. 2nd Joint EMBS/BMES Conf.*, vol. 3, 2002, pp. 2356–2357.

[13] J. M. Hollerbach, "Locomotion interfaces," in *Handbook of Virtual Environments: Design, Implentation, and Applications*, K. M. Stanley, Ed. Mahwah, NJ: Lawrence Erlbaum, 2002, pp. 239–254.

[14] N. Shiozawa, S. Arima, and M. Makikawa, "Virtual walkway system and prediction of gait mode transition for the control of the gait simulator," in *Proc. 26th Annu. Int. Conf. IEEE EMBS*, San Francisco, CA, Sep. 2004, pp. 2699–2702.

[15] G. Colombo, M. Joerg, R. Schreier, and V. Dietz, "Treadmill training of paraplegic patients with a robotic orthosis," *J. Rehab. Res. Devel.*, vol. 37, no. 6, pp. 693–700, 2000.

[16] M. Visintin, H. Barbeau, N. Korner-Bitensky, and N. Mayo, "A new approach to retrain gait in stroke patients through body weight support and treadmill stimulation," *Stroke*, vol. 29, pp. 1122–1128, 1998.

[17] V. R. Edgerton, R. D. Leon, S. J. Harkema, J. A. Hodgson, N. London, D. J. Reinkensmeyer, R. R. Roy, R. J. Talmadge, N. J. Tillakaratne, W. Timoszyk, and A. Tobin, "Retraining the injured spinal cord," *J. Physiol.*, vol. 533 (Pt. 1), pp. 15–22, May 2001.

[18] S. Hesse, C. Werner, S. v. Frankenberg, and A. Bardeleben, "Treadmill training with partial body weight support after stroke," *Phys. Med. Rehab. Clin. N. Am.*, vol. 14, no. 1 (Suppl.), pp. S111–S123, 2003.

[19] M. Maegele, S. Muller, A. Wernig, V. R. Edgerton, and S. J. Harkema, "Recruitment of spinal motor pools during voluntary movements versus stepping after human spinal cord injury," *J. Neurotrauma*, vol. 19, no. 10, pp. 1217–1229, 2002.

[20] S. Hesse and D. Uhlenbrock, "A mechanized gait trainer for restoration of gait," *J. Rehab. Res. Devel.*, vol. 37, no. 6, pp. 701–708, 2000.

[21] S. Jezernik, G. Colombo, and M. Morari, "Automatic gait-pattern adaptation algorithms for rehabilitation with a 4-DOF robotic orthosis," *IEEE Trans. Robot. Autom.*, vol. 20, no. 3, pp. 574–582, Jun. 2004.

[22] D. J. Reinkensmeyer, J. H. Wynne, and S. J. Harkema, "A robotic tool for studying locomotor adaptation and rehabilitation," in *Proc. 2nd Joint Meeting IEEE Eng. Med. Biol. Soc. Biomed. Eng. Soc.*, Houston, TX, Oct. 2002, pp. 2353–2354.

[23] J. A. Galvez, G. Kerdanyan, S. Maneekobkunwong, R. Weber, M. Scott, S. J. Harkema, and D. J. Reinkensmeyer, "Measuring human trainers' skill for the design of better robot control algorithms for gait training after spinal cord injury," in *Proc. Int. Conf. Rehab. Robot.*, Chicago, IL, 2005, pp. 231–234.

[24] R. Shadmehr and F. A. Mussa-Ivaldi, "Adaptive representation of dynamics during learning of a motor task," *J. Neurosci.*, vol. 14, no. 5 (Pt. 2), pp. 3208–3224, 1994.
[25] D. J. Reinkensmeyer, J. L. Emken, J. Liu, and J. E. Bobrow. The nervous system appears to minimize a weighted sum of kinematic error, force, and change in force when adapting to viscous environments during reaching and stepping. presented at *Adv. Computat. Motor Control III*. [Online]. Available: http://www.bme.jhu.edu/acmc
[26] J. L. Emken and D. J. Reinkensmeyer, "Robot-enhanced motor learning: Accelerating internal model formation during locomotion by transient dynamic amplification," *IEEE Trans. Neural Syst. Rehab. Eng.*, vol. 13, no. 1, pp. 33–39, Jan. 2005.

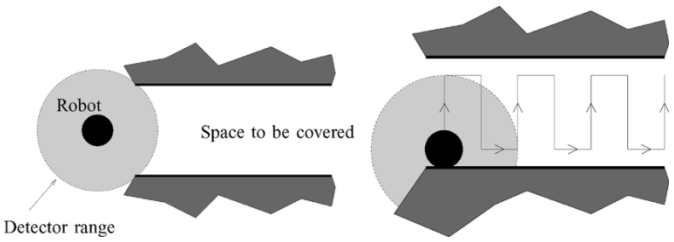

Fig. 1. Robot is required to pass the extended-range detector over all the points in the corridor. Even though the robot can perform back-and-forth motions to cover the space, these motions will not make efficient use of the available detector range.

Sensor-Based Coverage With Extended Range Detectors

Ercan U. Acar, Howie Choset, and Ji Yeong Lee

***Abstract*—Coverage path planning determines a path that passes a robot, a detector, or some type of effector over all points in the environment. Prior work in coverage tends to fall into one of two extremes: coverage with an effector the same size of the robot, and coverage with an effector that has infinite range. In this paper, we consider coverage in the middle of this spectrum: coverage with a detector range that goes beyond the robot, and yet is still finite in range. We achieve coverage in two steps: The first step considers vast, open spaces, where the robot can use the full range of its detector; the robot covers these spaces as if it were as big as its detector range. Here we employ previous work in using Morse cell decompositions to cover unknown spaces. A cell in this decomposition can be covered via simple back-and-forth motions, and coverage of the vast space is then reduced to ensuring that the robot visits each cell in the vast space. The second step considers the narrow or cluttered spaces where obstacles lie within detector range, and thus the detector "fills" the surrounding area. In this case, the robot can cover the cluttered space by simply following the generalized Voronoi diagram (GVD) of that space. In this paper, we introduce a hierarchical decomposition that combines the Morse decompositions and the GVDs to ensure that the robot indeed visits all vast, open, as well as narrow, cluttered, spaces. We show how to construct this decomposition online with sensor data that is accumulated while the robot enters the environment for the first time.**

***Index Terms*—Cell decomposition, coverage, Morse decomposition, sensor-based planning, Voronoi diagrams.**

I. Introduction

Coverage path planning determines a path that directs a robot to pass over all points in its free space. Integrating the robot's footprint (detector range) along the coverage path yields an area identical to that of the target region. We achieve coverage by introducing new types of *exact cell decompositions*. Exact cell decompositions [8], [16] represent the free space by dividing it into nonoverlapping regions called *cells*, such that adjacent cells share a common boundary, the interior of each cell intersects no other cell, and the union of all of the cells fills the free space. An adjacency graph encodes the topology of the cell decomposition, where nodes represent the cells and edges connect nodes corresponding to adjacent cells. Cell decompositions have conventionally been used to determine a path between two points which can be solved in two steps: first, identify the cells containing the start and the goal, and then search the adjacency graph for a sequence of cells that connect the start cell to the goal cell.

We use cell decompositions, however, to produce a path that *covers* the free space. We define cell boundaries such that each cell can be covered via a simple pattern, such as simple back-and-forth motions. A planner achieves complete coverage simply by ensuring that the robot identifies and visits each cell in the space, which is equivalent to finding an exhaustive walk through the adjacency graph.

In previous work, we defined a family of cell decompositions termed *Morse decompositions*, whose cells are defined by critical points of a Morse function. This work was motivated by Canny's roadmap work [5] where he uses critical points to ensure the connectivity of his roadmap. The critical points serve as landmarks because topologically meaningful events occur at them. Recall that Morse functions are real-valued functions with nondegenerate critical points. The Morse decompositions allow us to design sensor-based coverage algorithms that use simple motions, such as back and forth, for coverage with a robot-size detector. Varying the Morse function that defines the decomposition changes the pattern by which coverage is achieved.

Now, consider two ends of the coverage spectrum: coverage with detectors the same size of the robot and infinite-range detectors. The Morse decompositions are suitable for coverage with detectors that are the same size of the robot; we call these robot-size detectors. If the robot has an infinite-range detector, then it need not use Morse decompositions. Instead, the robot can follow the generalized Voronoi diagram (GVD) (sets of points equidistant to two obstacles [11], [19]) to completely cover a bounded free space.

In this paper, we address a problem in the middle of the extremes. We describe a new method to cover unknown spaces with detectors, such as infrared imaging systems or omnidirectional cameras, whose ranges are larger than the robot, but are still less than infinite. We term these *extended-range detectors.* In a sense, an extended-range detector has a "variable" effector size: in a vast, open space, the maximum range of the detector is the effector size. Covering a vast, open space with back-and-forth motions, as if the robot were as big as its maximum detector range, produces a "good" coverage path when the objective is to minimize path length with respect to the area covered.

In narrow spaces, however, the detector's range is limited by the presence of obstacles. As suggested in previous work by Hert *et al.* [14], and then by Lumelsky *et al.* [17], performing simple back-and-forth motions, again as if the robot were as big as its maximum detector range, does not produce an efficient path (Fig. 1). When the robot is in a cluttered or narrow space, its detector is effectively infinite, and thus can cover the space as if it had an infinite detector. See Fig. 2 for an overview of three modes of coverage: robot-size detector, extended-range detector, and infinite-range detector.

Manuscript received October 15, 2004; revised April 15, 2005. This paper was recommended for publication by Associate Editor G. Oriolo and Editor I. Walker upon evaluation of the reviewers' comments.

E. U. Acar was with the Robotics Institute, Department of Mechanical Engineering, Carnegie Mellon University, Pittsburgh, PA 15213 USA. He is now with Intel Research, Hillsboro, OR 97124 USA (e-mail: acar@cmu.edu).

H. Choset is with the Robotics Institute, Department of Mechanical Engineering, Carnegie Mellon University, Pittsburgh, PA 15213 USA (e-mail: choset@cs.cmu.edu).

J. Y. Lee is with the Korea Institute of Science and Technology, Seoul 136-791, Korea (e-mail: jiyeongl@andrew.cmu.edu).

Digital Object Identifier 10.1109/TRO.2005.861455